

Missing large-angle correlations versus even-odd point-parity imbalance in the cosmic microwave background

M.-A. Sanchis-Lozano¹, F. Melia^{2*}, M. López-Corredoira³ and N. Sanchis-Gual⁴

¹Instituto de Física Corpuscular (IFIC) and Departamento de Física Teórica, Centro Mixto Universitat de València-CSIC, Dr. Moliner 50, E-46100 Burjassot, Spain; e-mail: Miguel.Angel.Sanchis@ific.uv.es

²Department of Physics, The Applied Math Program, and Department of Astronomy, The University of Arizona, Tucson, Arizona 85721, USA; e-mail: fmelia@email.arizona.edu

³Instituto de Astrofísica de Canarias, E-38205 La Laguna, Tenerife, Spain

Departamento de Astrofísica, Universidad de La Laguna, E-38206 La Laguna, Tenerife, Spain; e-mail: fuego.templado@gmail.com

⁴Departamento de Matemática da Universidade de Aveiro and Centre for Research and Development in Mathematics and Applications (CIDMA), Campus de Santiago, 3810-183 Aveiro, Portugal

Received September 24, 2021

ABSTRACT

Context. The existence of a maximum correlation angle ($\theta_{\max} \gtrsim 60^\circ$) in the two-point angular temperature correlations of cosmic microwave background (CMB) radiation, measured by WMAP and *Planck*, stands in sharp contrast to the prediction of standard inflationary cosmology, in which the correlations should extend across the full sky (i.e., 180°). The introduction of a hard lower cutoff (k_{\min}) in the primordial power spectrum, however, leads naturally to the existence of θ_{\max} . Among other cosmological anomalies detected in these data, an apparent dominance of odd-over-even parity multipoles has been seen in the angular power spectrum of the CMB. This feature, however, may simply be due to observational contamination in certain regions of the sky.

Aims. In attempting to provide a more detailed assessment of whether this odd-over-even asymmetry is intrinsic to the CMB, we therefore proceed in this paper, first, to examine whether this odd-even parity imbalance also manifests itself in the angular correlation function and, second, to examine in detail the interplay between the presence of θ_{\max} and this observed anomaly.

Methods. We employed several parity statistics and recalculated the angular correlation function for different values of the cutoff k_{\min} in order to optimize the fit to the different *Planck* 2018 data.

Results. We find a phenomenological connection between these features in the data, concluding that both must be considered together in order to optimize the theoretical fit to the *Planck* 2018 data.

Conclusions. This outcome is independent of whether the parity imbalance is intrinsic to the CMB, but if it is, the odd-over-even asymmetry would clearly point to the emergence of new physics.

Key words. cosmological parameters – cosmology: cosmic background radiation – cosmology: observations – cosmology: theory – large-scale structure of the Universe

1. Introduction

As is well known, observations of the temperature fluctuations in the cosmic microwave background (CMB) radiation show that our Universe is quite uniform on scales much larger than the apparent (or Hubble) horizon (Melia 2018) at the time of decoupling. According to standard cosmology, this so-called horizon problem can be overcome by assuming an inflationary phase lasting a tiny fraction of a second almost immediately after the Big Bang (Starobinsky 1979; Kazanas 1980; Guth 1981; Linde 1982). Meanwhile, quantum fluctuations in the underlying inflaton field ϕ (Mukhanov 2005) would have grown and (somehow) classicalized to produce density perturbations that were also stretched enormously by the accelerated expansion, eventually forming the seeds of today's large-scale structure, including galaxies and clusters (Peebles 1980). Inflation has also been invoked to explain why the Universe today appears to be spatially flat, if the initial spatial curvature was indeed set arbitrarily (but see Melia 2022). If this initial condition were truly indeterminate, the Universe would have required an astonishing

degree of fine-tuning at the time of the Big Bang to evolve into what we see today without the effects of inflation.

The most popular inflation models tend to adopt the slow-roll condition, positing that the inflaton potential $V(\phi)$ changed very slowly during the phase of exponentiated expansion. For these scenarios, it is convenient to measure the inflation time as a function of the number of e-folds, N_e , in the expansion factor $a(t)$. The duration of inflation would then be roughly equal to $N_e H_\phi^{-1}$, where $H_\phi \equiv \dot{a}/a$ was the Hubble parameter at that time. In principle, the horizon and flatness problems might both be solved by requiring an inflation corresponding to $N_e \gtrsim 60$, one of the more notable successes of the inflation paradigm.

As we show below, however, the existence of a maximum correlation angle ($\theta_{\max} \gtrsim 60^\circ$) observed in the CMB by all three major satellite missions, COBE (Hinshaw et al. 1996), WMAP (Bennett et al. 2003), and *Planck* (Planck Collaboration 2018), implies a smaller number of e-folds ($N_e \approx 55$), contrasting with most inflationary scenarios (Melia & López-Corredoira 2017; Liu & Melia 2020; Melia et al. 2021). Moreover, this discrepancy does not stand in isolation. Many other puzzles and anomalies contributing to an increasing level of tension with standard

Send offprint requests to: M.-A. Sanchis-Lozano

* John Woodruff Simpson Fellow

cosmology (Λ CDM) have emerged in recent years as the accuracy of the observations has improved (see, e.g., the recent review by Perivolaropoulos & Skara 2021). For example, Schwarz et al. (2016) included in their list of CMB anomalies an apparent alignment of the lowest multipole moments with each other and with the motion and geometry of the Solar System, a hemispherical power asymmetry, and an unexpectedly large cold spot in the southern hemisphere. Di Valentino et al. (2021) argued against general concordance by demonstrating that a combined analysis of the CMB angular power spectrum obtained by *Planck* and the luminosity distance inferred simultaneously from type Ia supernovae (SNe) excludes a flat universe and a cosmological constant at the 99% confidence level. A broader view of the general tension between the predictions of Λ CDM and the observations may be found in López-Corredoira (2017). Whether some of these anomalies have a common origin becomes of paramount importance to the fundamental basis of our cosmological modeling.

In this paper we focus on two of the more recent discrepancies. The first is the lack of large-angle correlations seen in the CMB data, which seems to suggest that the primordial power spectrum, $\mathcal{P}(k)$, had a hard cutoff at a k_{\min} distinctly different from zero. This explanation for the angular-correlation anomaly has recently been shown to also account self-consistently for the missing power at low ℓ s in the angular power spectrum (Melia et al. 2021). This feature in $\mathcal{P}(k)$ indicates the time at which inflation could have started (Liu & Melia 2020), hence setting an upper limit to the possible number of e-folds by the time it ended. It is k_{\min} that now appears to create an inconsistency between the number of e-folds required to solve the horizon problem and that corresponding to the measured fluctuation spectrum (Melia & López-Corredoira 2017). The second is an apparent preference of the CMB data for an odd point-parity, first inferred from the analysis of the angular power spectrum (see, e.g., Kim et al. 2012; Schwarz et al. 2016). We seek to confirm whether this odd-even imbalance is also present in the measured angular correlation function, and if it is, we attempt to find a phenomenological connection between these two recently identified features in the CMB fluctuation distribution.

We note, however, that an interpretation of the odd-even imbalance as being intrinsic to the CMB anisotropies is not universally accepted. For example, Creswell & Naselsky (2021a) suggested that this asymmetry may be due to a contamination from a few regions of the sky. We return to this viable possibility toward the end of our discussion in § 4. The work we carry out in this paper can therefore provide a more quantitative assessment of the idea that the an odd-even imbalance may originate within the CMB anisotropies for a more detailed comparison with the alternative scenario in which it is primarily due to some observational contamination. In doing so, we attempt to answer the questions whether (i) either one or the other of these characteristics is sufficient to account for the observed angular correlation function, or if are both required; and (ii) if the latter is true, whether the reoptimized value of k_{\min} is different from that reported earlier (Melia & López-Corredoira 2017; Melia et al. 2021) and might mitigate the current level of tension between the latest *Planck* release and the predictions of standard inflationary cosmology.

In this paper, we do not, however, include the potentially useful information concerning the polarization of the CMB radiation available from *Planck* for several practical reasons. The E-mode polarization arising from the Thomson scattering of photons by free electrons is dominated by optically thin plasma on small spatial scales. Therefore, these polarization effects cannot extend over large angular scales. In addition, the subtraction of

foreground contamination is more difficult to carry out for polarized CMB light based on the current *Planck* data because of the required complex multicomponent fitting. Future missions such as *Litebird* (Errard et al. 2016), *PICO* (Hanany et al. 2019) and *COrE* (Bouchet et al. 2011) will achieve more precise measurements at much higher sensitivity than is currently available with *Planck*, and should be able to answer the question of whether the large-angle anomalies seen in the temperature fluctuations are confirmed by the polarization maps.

2. Angular correlations in the CMB

One of the main goals of analyzing the angular correlation function of the CMB is to extract information regarding the different stages of the evolution of the Universe. Based on very general grounds, small (large) angles between CMB photon trajectories can be associated with small (large) length scales in the source plane (the opposite of using energy scales). Furthermore, it offers us the possibility of analyzing an important assumption in Λ CDM, that is, that the fluctuations are Gaussian and statistically homogeneous and isotropic. As previously noted, the angular correlation function of the CMB is already known to exhibit several statistical anomalies. In this section, we focus on the lack of large-angle correlations, but we first recall features in the CMB that are of special interest to this study.

It is customary to distinguish primary anisotropies arising prior to decoupling, from *secondary* anisotropies developed as the CMB photons propagate from the last scattering surface to the observer. We do not distinguish between recombination, last scattering surface, or freeze-out times, but approximate all of them as equal to a cosmic time $t_d \approx 3.8 \times 10^5$ years ($z \approx 1100$). For angles greater than a few degrees, the primary contributor to the former is the Sachs-Wolfe (SW) effect (Sachs & Wolfe 1967), representing fluctuations in the metric leading to temperature anisotropies via perturbations of the gravitational potential at the time of decoupling. There are two Sachs-Wolfe influences: the above-mentioned, nonintegrated Sachs-Wolfe effect, and the integrated Sachs-Wolfe effect (ISW). The latter is sometimes also further subdivided into an early ISW (taking place just after decoupling; for convenience, this is often just included in the SW), and a late ISW, arising while the CMB photons propagated through the expanding medium. The ISW contributes non-negligibly to the CMB anisotropies only if the universal expansion is at least partially driven by something other than purely nonrelativistic matter. In the standard model, dark energy—possibly in the form of a cosmological constant—started influencing the expansion at $z \sim 0.5$, corresponding to a cosmic time ~ 10 Gyr. The ISW has the effect of mainly raising the Sachs plateau at low multipoles. However, the detection of this ISW due to dark energy is not fully confirmed yet. The putative detections may simply be noise with underestimated error bars (López-Corredoira et al. 2010; Dong et al. 2021).

A way to address the angular dependence and anisotropies of the CMB is through its primary power spectrum, originally defined by the Fourier transform of the primordial fluctuation spectrum, usually parameterized as

$$P(k) = A \left[\frac{k}{k_0} \right]^{n_s - 1}, \quad (1)$$

where n_s is the scalar spectral index. The spectrum would be perfectly scale free (with $n_s = 1$) if the Hubble parameter H_ϕ were strictly constant during inflation. In typical slow-roll inflationary models, however, this is only approximately true, and

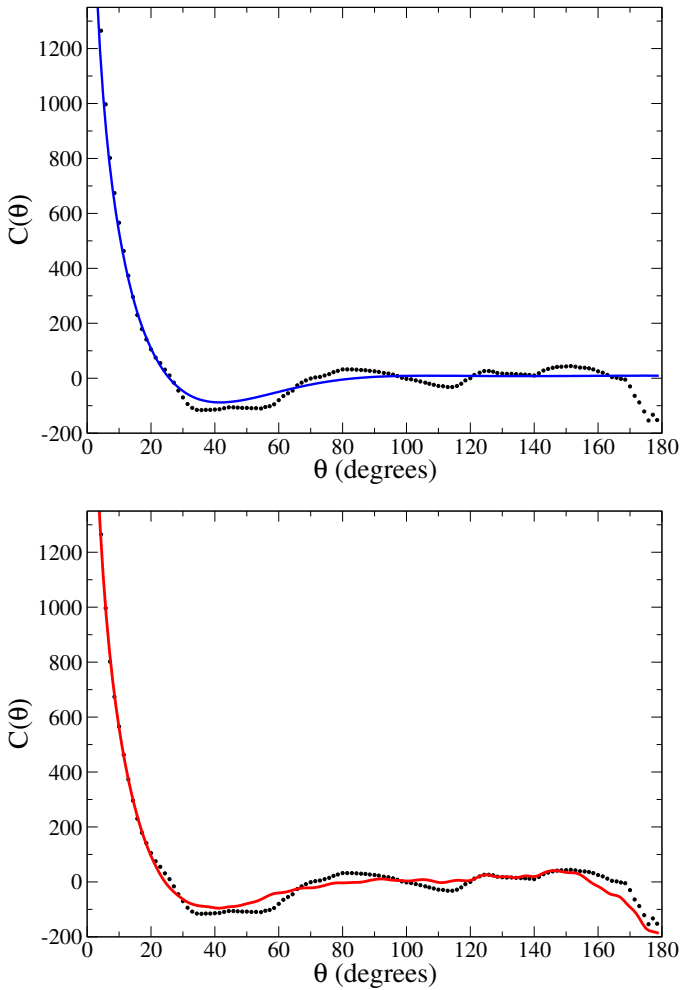


Fig. 1. Two-point correlation function $C(\theta)$ (solid curves) optimized to fit the *Planck* 2018 data (black points) (Planck Collaboration 2018). (a) Top panel: $u_{\min} = 4.5$ and odd-even parity balance of multipoles (blue curve). (b) Bottom panel: $u_{\min} = 4.5$ and odd-even parity dominance (red curve). See main text.

H_ϕ evolves slowly, which produces a slight deviation of the spectral index from one. The observations show that in fact $n_s = 0.9649 \pm 0.0042$ (Planck Collaboration 2018), adding some observational support for a slow-roll potential, $V(\phi)$.

2.1. Two-point angular correlation function

The anisotropies in the CMB are very small, of about one part in 10^5 , but they carry a wealth of information pertaining to the possible influence of $V(\phi)$ and the subsequent evolution of the Universe after reheating. A very powerful probe of these fluctuations is the two-point angular correlation function, defined as the ensemble product of the temperature differences with respect to the average temperature, from two directions in the sky defined by unitary vectors \mathbf{n}_1 and \mathbf{n}_2 ,

$$C(\theta) = \langle T(\mathbf{n}_1)T(\mathbf{n}_2) \rangle. \quad (2)$$

The angle $\theta \in [0, \pi]$ is defined by the scalar product $\mathbf{n}_1 \cdot \mathbf{n}_2$.

One typically expands $C(\theta)$ in terms of Legendre polynomials (assuming azimuthal symmetry)

$$C(\theta) = \frac{1}{4\pi} \sum_{\ell=2}^{\infty} (2\ell + 1)C_\ell P_\ell(\cos \theta), \quad (3)$$

where the C_ℓ coefficients encode the information with cosmological significance from the sky. The sum starts at $\ell = 2$ and ends at a given ℓ_{\max} , dictated by the resolution of the data. The first two terms are excluded because (i) the monopole ($\ell = 0$) is simply the average temperature over the whole sky and plays no role in the correlations, other than a global scale shift; and (ii) the dipole ($\ell = 1$) is greatly affected by Earth's motion, creating an anisotropy that dominates the intrinsic cosmological dipole signal.

2.2. Maximum angle in two-point angular correlations

Large-angle correlations in the CMB provide information about the earliest stages of the primitive Universe, well before recombination and the subsequent formation of cosmic structure. In this context, it may be useful to point out an interesting analogy with the angular correlations among the final-state particles in heavy-ion or proton-proton collisions at the Large Hadron Collider, and the early formation of nonconventional matter, such as a quark-gluon plasma or hidden valley particles (Sanchis-Lozano et al. 2020). In Figure (1a) we plot the observed angular correlation function (black dots) measured by *Planck* (Planck Collaboration 2018), compared with fitted (blue and red) curves to be discussed below. Above $\simeq 60^\circ$, the correlations drop to near zero, except for a downward tail at $\sim 180^\circ$, which we also examine in more detail below. This shape of $C(\theta)$, particularly its suppression at large angles, was unexpected in standard cosmology, given that inflation was supposed to begin early enough (with $k_{\min} \rightarrow 0$) to provide the required number of e-folds to solve the horizon and flatness problems, thereby providing coverage across the full sky (see, e.g., Melia 2014).

It is worth mentioning at this point that these expectations on the value of k_{\min} and correlations at all angles are primarily based on the correctness of the standard model. Large-angle correlations are not necessarily expected in all cosmological models, however. For example, in the alternative cosmology known as the $R_h = ct$ universe, which does not have an inflationary epoch, the expansion factor is linear in time and the maximum angle corresponds to the size of the apparent horizon (Melia 2018) at decoupling,

$$\theta_{\max} \simeq \frac{2\pi}{\ln(t_0/t_d)} \quad (\text{in radians}), \quad (4)$$

where t_d and t_0 denote the decoupling and present cosmic times, respectively. The $R_h = ct$ universe is an FLRW cosmology in which the equation of state is constrained by the zero active mass condition in general relativity, that is, $\rho + 3p = 0$. The Raychaudhuri equation clearly shows that $\ddot{a} = 0$ in that case, which leads to a Universe expanding at a constant rate (Melia 2013a). This Universe has no horizon problem, and spatial flatness is ensured because the total energy density is zero. It therefore has no need for inflation. In such a universe, the Hubble parameter is always exactly equal to the inverse of the age of the Universe, and the Hubble radius satisfies $R_h = ct$ at all times, hence the eponymous origin of its name. Setting $t_d = 3.8 \times 10^5$ years and $t_0 = 13.8$ Gyr, we obtain $\theta_{\max} \sim 40^\circ$. Thus, if inflation were to fail to adequately explain the existence of such a maximum correlation angle, it might be considered evidence supporting a noninflationary model, such as $R_h = ct$.

We generalize the expression in Equation (4) by writing it in terms of the maximum fluctuation size $\lambda_{\max}(t_d)$ at decoupling time t_d and the proper distance $R_d \equiv a(t_0)r_d$ (with r_d the comov-

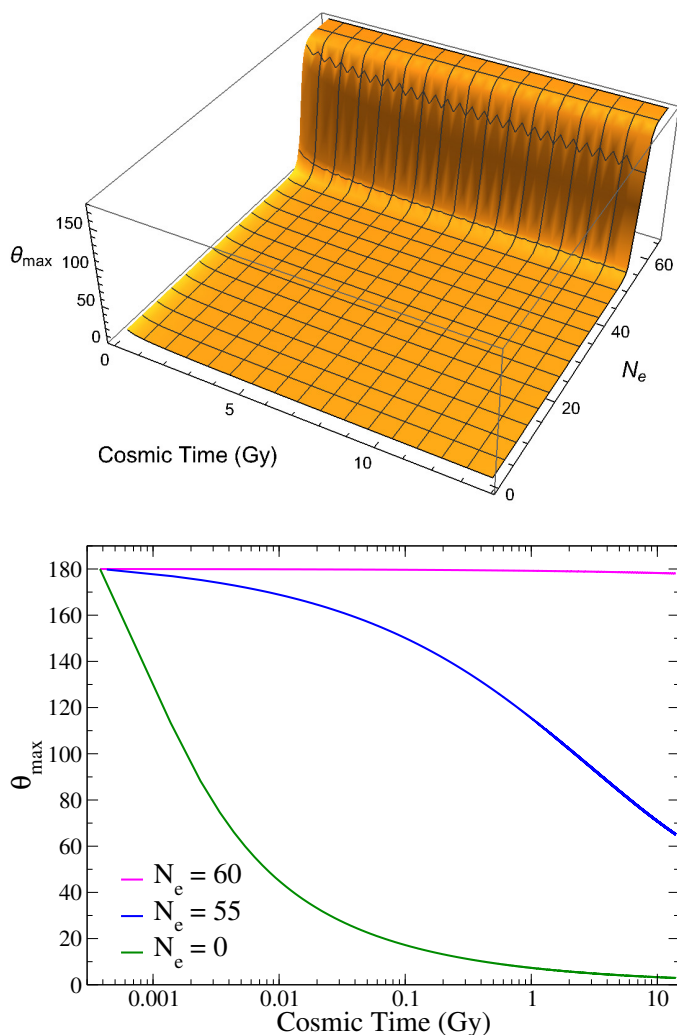


Fig. 2. Maximum correlation angle due to inflation. Top panel (a): 3D plot of the maximum correlation angle as a function of cosmic time and the number of e-folds. Bottom panel (b): Maximum correlation angle evolution with cosmic time for different N_e values, corresponding to vertical sections in the 3D plot. We highlight that the plateau for N_e is smaller than about 50, implying a large inhomogeneity of the CMB along cosmic time.

ing distance) from us to the last scattering surface,

$$\theta_{\max} = 2 \tan^{-1} \left[\frac{\lambda_{\max}}{R_d} \right]. \quad (5)$$

Because we study the formation of primordial physical quantities, the apparent horizon (equal to the Hubble radius in this case) should set the basic length scale at stake (Melia 2013b, 2020b). In particular, the maximum fluctuation size can be estimated as $\lambda_{\max} = \alpha 2\pi R_h$, where $\alpha \lesssim 1$ denotes a coefficient dependent on the cosmological model. For instance, $\alpha = 1$ for de Sitter space and $\alpha \simeq 0.5$ for Λ CDM (Melia 2013b, 2018). This scale changes as the expansion factor $a(t)$ grows, starting with the assumed slow-roll inflation, followed by radiation and then matter-dominated evolution, before reaching decoupling, where the CMB radiation was released. Nevertheless, knowledge of R_h at decoupling is sufficient to estimate λ_{\max} associated with the largest fluctuation we can see in the CMB anisotropies today.

On the other hand, to compute the proper distance R_d between us and the last scattering surface, we must know the ex-

pansion history from decoupling to today. An excellent approximation for $a(t)$ during this time may be written

$$a(t) \sim \sinh^{2/3}(\tilde{H} t), \quad (6)$$

where $\tilde{H} \equiv (3/2) \sqrt{\Omega_\Lambda} H_0$, with Ω_Λ and H_0 denoting the normalized dark matter density and Hubble constant today, respectively, and t the cosmic time since the Big Bang (see Appendix A).

In Figure 2 we show the maximum correlation angle obtained in our study under different assumptions concerning the inflationary epoch. Figure 2(a) shows a 3D rendition of the maximum correlation angle as a function of cosmic time and the number of e-folds (N_e). The correlation angle remains confined to just a few degrees for any number of e-folds $N_e \lesssim 40$. For $N_e \geq 62$, on the other hand, the curve quickly reaches 180° along the whole cosmic time until now. For the sake of clarity, the maximum correlation angle evolution with cosmic time is shown in Figure 2(b) for different N_e values, corresponding to vertical cuts in the 3D plot (Fig. 2a) (see Appendix A for the mathematical details).

The late-time ISW effect yielding additional secondary anisotropies should tend to broaden the angular correlations as lower- ℓ multipoles are enhanced (due to a raising of the Sachs-plateau). Therefore, the number of e-folds required to comply with the observed maximum value of θ_{\max} should decrease even further once the ISW is taken into account. The *Planck* 2018 data therefore suggest that $N_e \lesssim 55$, creating even greater tension with the conventional slow-roll inflationary scenario. Liu & Melia (2020) provided more details concerning the difficulties faced by the slow-roll paradigm to simultaneously solve the horizon problem and missing correlations at large angles.

Addressing these constraints from the latest CMB data would require a more complicated inflationary process than is usually conjectured. As we show below, this conclusion goes in the same direction as the need for a cutoff in the power spectrum in order to correctly reproduce the whole angular correlation function of the CMB.

2.3. Low cutoff in the CMB power spectrum

Λ CDM predicts an angular correlation curve that crosses the zero-axis twice and extends over the whole 180° range of poloidal angles (see, e.g., Fig. 1 in Melia 2014). This result is manifestly inconsistent with observational evidence, which shows a maximum correlation angle of $\geq 60^\circ$, as already discussed in the previous section.

In order to mitigate this tension, Melia & López-Corroira (2017) introduced a cutoff to the primordial power spectrum, representing a lower limit to the integral

$$C_\ell = N \int_{k_{\min}}^{\infty} dk k^{n_s-1} j_\ell^2(k r_d), \quad (7)$$

where the normalization constant N and the minimum mode wavenumber k_{\min} are optimized using a global fit to the whole observed angular correlation function. Although this procedure represents a phenomenological introduction of the cutoff k_{\min} , this truncation has some theoretical justification in that it represents the first quantum fluctuation to either (i) have crossed the Hubble horizon once inflation started, or (ii) have emerged out of the Planck domain if inflation never happened (see Melia 2019; Liu & Melia 2020). The need for a k_{\min} may also be related to the infrared regularization of the inflaton field commutator, although in standard cosmology, it should then likely be much smaller than its value (i.e., $\simeq 3 \times 10^{-4} \text{ Mpc}^{-1}$, corresponding to

$u_{\min} = 4.34$) optimized using the *Planck* 2018 data (Liu & Melia 2020).

In the computation of the C_ℓ coefficients, only the SW effect is taken into account, ignoring other effects such as the baryon acoustic oscillations (BAO), whose influence extends primarily over smaller angles ($\theta \lesssim 5^\circ$) and hence only the very large- ℓ multipoles (certainly > 100). Changing the integration variable from k to $u \equiv kr_d$ in Equation (7) and setting $n_s = 1$ for simplicity, we obtain

$$C_\ell = N \int_{u_{\min}}^{\infty} du \frac{j_\ell^2(u)}{u}. \quad (8)$$

We point out that only those C_ℓ coefficients with $\ell \lesssim 20$ are actually affected by the existence of the cutoff u_{\min} in the above integral.

In a previous computation of these coefficients using the *Planck* 2103 dataset, Melia & López-Corredoira (2017) found that the best fit to the angular correlation function is obtained with $u_{\min} = 4.34 \pm 0.50$, which translates into a minimum wavenumber $k_{\min} = 4.34/r(t_d)$ (see also the similar limit placed on k_{\min} by an analogous study of the angular power spectrum itself; Melia et al. 2021). In the present paper, we repeated this analysis using the more recent *Planck* 2018 dataset, obtaining $u_{\min} = 4.5 \pm 0.5$, and $k_{\min} = 4.5/r(t_d)$, which is compatible with the previous results from *Planck* 2013. We provide more details about the statistical analysis yielding this result below.

Very importantly, an almost zero correlation plateau above the maximum angle ($\theta_{\max} \approx 60^\circ$) can be obtained by setting a lower cutoff to the integration variable u , corresponding to a lower cutoff in the power spectrum. Mathematically, this result can be understood as a delicate balance between even and odd multipole contributions to $C(\theta)$. We return to this crucial point in the next section.

3. Odd versus even point-parity in the CMB

Among the other anomalies observed in the CMB, an odd-even parity violation may indicate a nontrivial topology of the Universe, unexpected physics at the pre- or inflationary epochs, or some unsolved systematic errors in the data reduction. In the following, we focus on the apparent odd-dominance of the CMB fluctuations, that is, the fact that the weight of odd multipoles in either the power spectrum or the two-point angular correlation function is larger than the corresponding weight of the even multipoles. This imbalance is commonly referred to as a point-parity asymmetry of the CMB, and we address two statistics below that are widely employed to analyze it.

3.1. Odd-even parity statistics

We employ the parity statistic (Panda et al. 2020)

$$P(\ell_{\max}) = \frac{P^+(\ell_{\max})}{P^-(\ell_{\max})}, \quad (9)$$

where

$$P^\pm(\ell_{\max}) = \sum_{\ell=2}^{\ell_{\max}} \gamma_\ell^\pm \frac{\ell(\ell+1)}{2\pi} C_\ell, \quad (10)$$

with the projectors defined as $\gamma_\ell^+ = \cos^2(\ell\pi/2)$ and $\gamma_\ell^- = \sin^2(\ell\pi/2)$. Assuming that $\ell(\ell+1)C_\ell$ is approximately constant at low ℓ , P^\pm can clearly be considered as a measurement of the

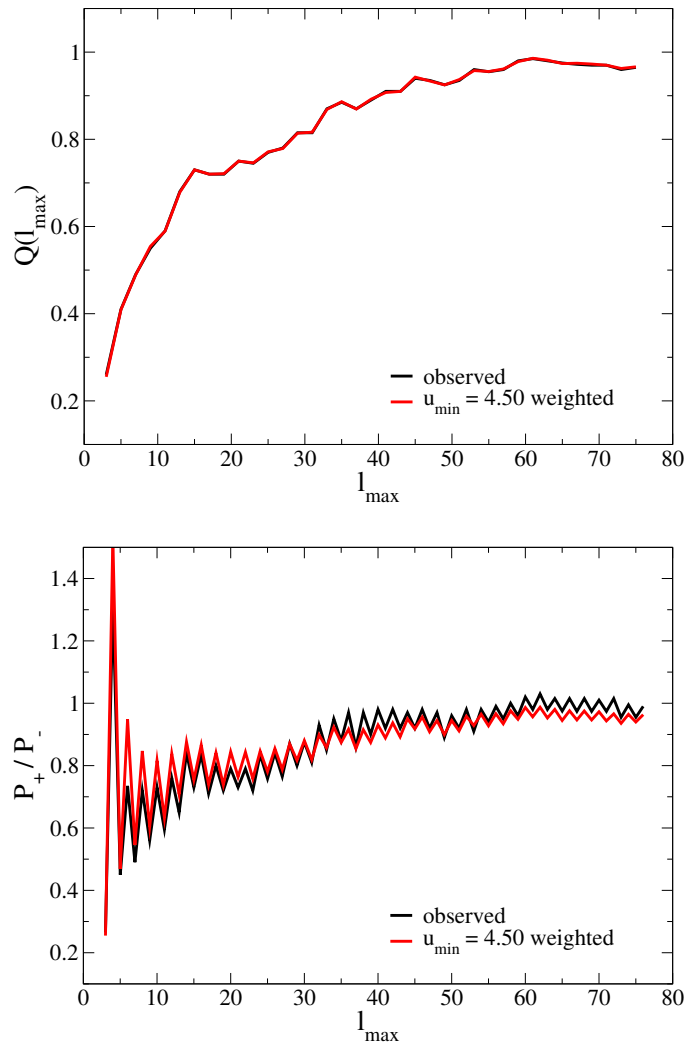


Fig. 3. Statistics used to describe the point-parity asymmetry of the CMB. (a) Top panel: $Q(\ell_{\max}^{\text{odd}})$ statistic as a function of ℓ_{\max} for $u_{\min} = 4.50$ (red), compared to the *Planck* 2018 data. The overlap is visually almost perfect. (b) Bottom panel: Same for the $P(\ell_{\max})$ statistic using the values of C_ℓ determined from the matching of the $Q(\ell_{\max}^{\text{odd}})$ statistic with the data shown on the left. The reduced χ^2 for this fit is $\chi_{\text{dof}}^2 \approx 0.99$.

degree of parity asymmetry: below unity, it implies odd-parity dominance, and vice versa. Any deviation of this statistic from unity points to an odd-even parity imbalance.

A second statistic useful for checking a point-parity imbalance may be defined as the average ratio of the power in adjacent odd and even multipoles up to a given ℓ value (Aluri & Jain 2012; Panda et al. 2020),

$$Q(\ell_{\max}^{\text{odd}}) = \frac{2}{\ell_{\max}^{\text{odd}} - 1} \sum_{\ell=3}^{\ell_{\max}^{\text{odd}}} \frac{D_\ell - 1}{D_\ell}, \quad (11)$$

where ℓ_{\max}^{odd} is the maximum odd multipole up to which the statistic is computed, and $D_\ell \equiv \ell(\ell+1)C_\ell/\pi$. In contrast to $P(\ell_{\max})$, the new statistic, $Q(\ell_{\max}^{\text{odd}})$, ensures that there are always the same number of odd and even powers along the whole considered multipole range, so no sawtooth oscillations are present. As for $P(\ell_{\max})$, this statistic is also expected to fluctuate about the value of one at low ℓ s.

In case of Gaussian fluctuations, the angular power spectrum and the angular correlation function contain the same informa-

tion concerning the angular distribution of temperature in the CMB. Nevertheless, although the angular power spectrum covers all of the ℓ dependence, it emphasizes large- ℓ values, such that most of the information at $\theta \gtrsim 10^\circ$ is squeezed into a very narrow interval, making it difficult to pick out any disagreement between theory and observation for the low multipoles. Conversely, the angular correlation function covers the fluctuation distribution more evenly over all angles, thereby making it relatively easier to study the large-angular region, corresponding to lower multipoles. Ultimately, both approaches should be mutually consistent as well as complementary for the extraction of useful information.

With this goal in mind, we require the statistic $Q(\ell_{\max}^{\text{odd}})$ (shown in red) to match (up to a given accuracy) the data (shown in black) in Figure 3(a). We do this by heuristically tuning the weights

$$q(\ell_{\text{even}}) = \frac{C_{\ell_{\text{even}}}}{C_{\ell_{\text{even}}+1}} \quad (12)$$

to optimize the fit. Then, using the above ratios, we fit the two-point angular correlation function keeping two parameters free, namely, the normalization, N , and the cutoff k_{\min} (i.e., u_{\min}). As noted earlier, the latter was already constrained to the interval $u_{\min} \in (4.34 \pm 0.50)$ in Melia & López-Corredoira (2017) using the old *Planck* 2013 data and without any consideration of a possible odd-even parity imbalance. We have carried out this analysis again for the latest *Planck* 2018 data at small, middle, and now large angles, incorporating the odd-parity dominance.

To incorporate these weights into the angular correlation function, we modified Equation (3) to read

$$C(\theta) = \frac{1}{4\pi} \sum_{\ell=2}^{\infty} (2\ell + 1) w_{\ell} C_{\ell} P_{\ell}(\cos \theta), \quad (13)$$

with

$$w_{\ell_{\text{even}}} = \frac{q(\ell_{\text{even}})}{q(\ell_{\text{even}}) + 1}, \quad w_{\ell_{\text{even}}+1} = 1 - w_{\ell_{\text{even}}}, \quad (14)$$

where ℓ_{even} denotes even values of ℓ within the selected interval. The weights w_{ℓ} for the coefficients C_{ℓ} , introduced ad hoc to model the odd-even imbalance, should not be confused with the window factors. Obviously, by requiring $q(\ell_{\text{even}}) \equiv 1 \forall \ell_{\text{even}}$, we obtain $w_{\ell_{\text{even}}} = w_{\ell_{\text{even}}+1} = 1/2$, thereby restoring the odd-even parity balance.

In Figure 3(a) we show the function $Q(\ell_{\max})$ for the *Planck* 2018 data (black) with the fit (red) corresponding to the set of parameters that provides the minimum reduced χ_{dof}^2 for the angular two-point correlations, keeping the cutoff we introduced to improve the fit (see Table 1). The matching of the observed and theoretical values achieved by tuning the ratios $q(\ell)$ (and their respective weighting factors, w_{ℓ}) that modify the C_{ℓ} coefficients is excellent. In addition, the set of weights optimized to find this match for $Q(\ell_{\max})$ also produces an excellent fit in the $P(\ell_{\max})$ plot, corresponding to a reduced χ_{dof}^2 near unity, as seen in Figure 3(b) and Table 1.

Figure 1(b) shows the plot of $C(\theta)$ over the whole range of angles with $u_{\min} = 4.5$, although this time, it incorporates the odd-dominance via the coefficients C_{ℓ} , modified as explained above. The fit now also matches the downward tail at large angles. To understand what is happening, consider the separate plots in Figure 4(a) that show the odd and even multipole contributions to $C(\theta)$. Each (odd and even) contribution behaves quite distinctly due to the intrinsic parity properties of the Legendre

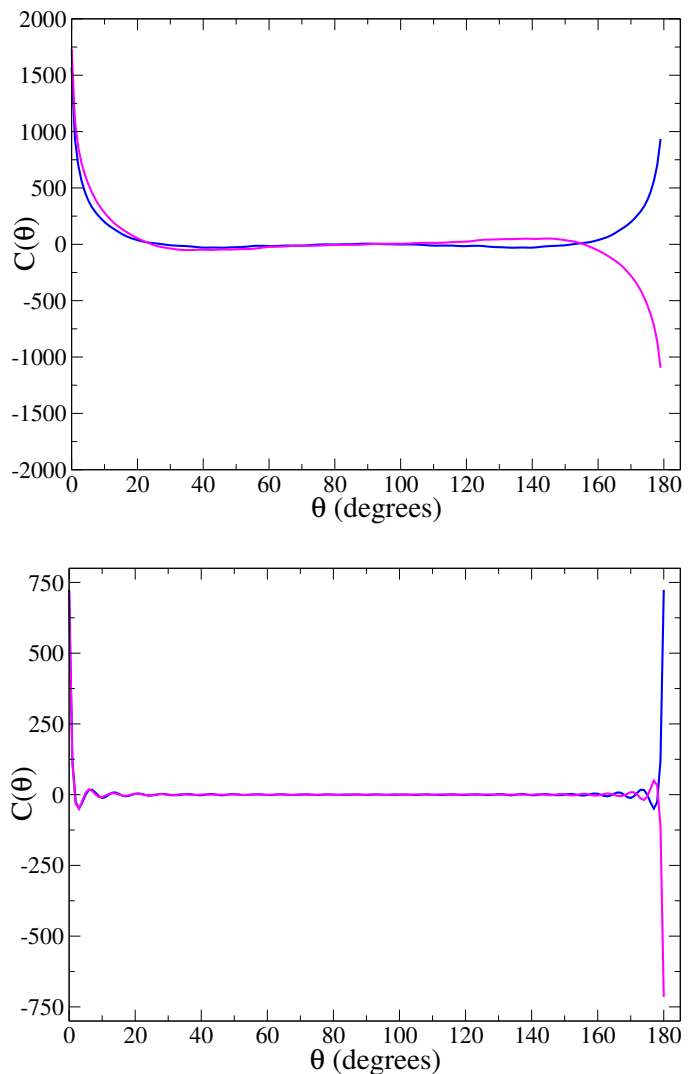


Fig. 4. Contributions from the even (blue) and odd (magenta) multipoles to the two-point angular correlation function $C(\theta)$ in Equation (13) for (a) $\ell \in [2, 401]$ (left panel) and (b) $\ell \in [40, 401]$ (right panel). The delicate balance between odd and even polynomials is clear even at high ℓ for large angles. Selecting a different weighting of each contribution has a strong influence on $C(\theta)$ at $\theta \approx 180^\circ$.

polynomials about $\theta = 90^\circ$. Consequently, once summed to produce the full $C(\theta)$, these two contributions produce constructive interference at small angles (i.e., $\theta < 90^\circ$) and destructive interference at large angles ($\theta > 90^\circ$).

One of our most important conclusions from this work is that in order to produce the optimum fit of the *Planck* 2018 data with the lowest χ_{dof}^2 in Figure 1(b), we must include in our theoretical $C(\theta)$ both the cutoff u_{\min} in Equation (8) and an odd-parity dominance via the weighting factors in Equation (13). Otherwise, our fit to the observed data points for either the angular correlation function or the parity statistics worsens considerably, yielding a χ_{dof}^2 much larger than one. Using both the cutoff ($k_{\min} \neq 0$) and an odd-even parity imbalance simultaneously produces the best fit for $C(\theta)$, $Q(\ell_{\max})$ and $P(\ell_{\max})$ (see Table 1), however.

As noted earlier, we find from our study an optimized cutoff $u_{\min} \approx 4.5 \pm 0.5$, in which the mean value and $\sigma = 0.5$ error were obtained using a Monte Carlo analysis to sample the

Table 1. χ^2_{dof} values for different fits to the two-point correlation function $C(\theta)$ and the parity statistic $P(\ell_{\text{max}})$, inferred from the *Planck* data. PB: parity balance; OD: odd dominance

Curve/parameters:	$u_{\text{min}} = 0+\text{PB}$	$u_{\text{min}} = 0+\text{OD}$	$u_{\text{min}} = 4.5+\text{PB}$	$u_{\text{min}} = 4.5+\text{OD}$
$C(\theta)$	6.1	3.8	0.80	0.70
$P(\ell_{\text{max}})$	30	5.3	18.0	0.99

variation of $C(\theta)$ within the measurement errors. Since the $C(\theta)$ points are highly correlated, we circumvented this problem using a Monte Carlo procedure as described in Melia & López-Corredoira (2017). Starting from 100 mock CMB catalogs, we computed the two-point correlation function $C_i(\theta)$, ($i = 1, 100$) in each case. From these, we obtained $\Delta C_i(\theta) = C_i(\theta) - C_0(\theta)$, where $C_0(\theta)$ is the angular correlation function in standard cosmology. Then we calculated $u_{\text{min},i}$ for $C(\theta) = C_{\text{Planck}}(\theta) + \Delta C_i(\theta)$ for each realization i . Next, from the resulting roughly Gaussian distribution of $u_{\text{min},i}$, we determined its average value and r.m.s., yielding $u_{\text{min}} \simeq 4.5 \pm 0.5$, whose corresponding χ^2_{dof} distribution from the $C(\theta)$ fits varies smoothly around its minimum at 4.5. This u_{min} range is slightly larger than but compatible with the interval obtained from the *Planck* 2013 dataset: $u_{\text{min}} = 4.34 \pm 0.50$.

A quantitative comparison of the various fits we have explored is provided in Table 1, which lists the χ^2_{dof} values for different choices of parameters, including the odd-even parity relative weights. A remark is in order: the improvement of the $C(\theta)$ fit, once $u_{\text{min}} = 4.5$ is fixed, is somewhat modest when passing from parity balance to parity breaking. This is easy to understand because the main effect of imposing odd-dominance takes place at large angles, where the observational uncertainties are quite large and its impact on the total χ^2_{dof} is thus relatively small. On the other hand, the agreement between the theoretical prediction and the parity statistic $P(\ell_{\text{max}})$ improves dramatically, as expected, given the observed odd-dominance, as seen in Figure 3(a).

We stress that the main benefit of using a $k_{\text{min}} \neq 0$ together with parity breaking is not so much the improvement of the fit to the two-point correlations (with a focus on the tail at large angles) at the cost of increasing the number of degrees of freedom, but the fact that this approach can simultaneously resolve several apparently disconnected anomalies in the CMB. The end result is an excellent fit of $C(\theta)$ at small, medium, and large angles (reproducing the existence of a $\theta_{\text{max}} \gtrsim 60^\circ$) with a p-value $\simeq 0.95$, and the implementation of an odd-parity dominance seen also in the angular power spectrum. This outcome constitutes the principal result of our analysis in this paper.

3.2. Relevance of the angular correlations at $\theta \simeq 180^\circ$

Large-angle correlations are commonly associated with low multipoles, typically $\ell \in [2, 20]$. We have already established that the introduction of a cutoff k_{min} mainly affects multipoles with $\ell \lesssim 20$, and significantly alters the shape of the $C(\theta)$ curve at $\theta \gtrsim 60^\circ$. In contrast, the net contribution of multipoles with $\ell \gtrsim 20$ practically cancels out, producing a plateau of zero correlation if nonuniform weights w_ℓ are excluded.

Nevertheless, the tail of $C(\theta)$ at $\theta \sim 180^\circ$ is influenced by the higher-order polynomials, even $\ell \gtrsim 20$. To demonstrate this effect, we have split the angular correlation function into two

pieces:

$$\begin{aligned}
 C(\theta) &= C(\theta; \ell \leq \ell_0) + C(\theta; \ell \geq \ell_0 + 1) \\
 &= \sum_{\ell=2}^{\ell_0} \frac{(2\ell+1)}{4\pi} w_\ell C_\ell P_\ell(\theta) + \\
 &\quad \sum_{\ell=\ell_0+1}^{\ell_{\text{up}}} \frac{(2\ell+1)}{4\pi} w_\ell C_\ell P_\ell(\theta). \tag{15}
 \end{aligned}$$

The first piece, $C(\theta; \ell \leq \ell_0)$, corresponds to the C_ℓ coefficients that are significantly affected by u_{min} in the integral of Equation (8) and the different odd-even weighting factors used to produce Figure 3(a). The second summation runs from $\ell_0 + 1$ up to $\ell_{\text{up}} = 401$ (ideally, infinity).

In contrast to conventional wisdom, the contribution of high- ℓ multipoles, $C(\theta; \ell \geq \ell_0 + 1)$, can certainly influence $C(\theta)$ even at angles $\theta \sim 180^\circ$. To see this, we separately plot in Figure 4(b) the contributions of even and odd multipoles for $\ell_0 > 40$. Due to the oscillatory behavior of the Legendre polynomials, both contributions add to always produce a positive correlation at smaller angles, while a delicate balance exists at $\theta \sim 180^\circ$ that yields zero correlation when the parity symmetry is exact. A slight imbalance between odd and even high- ℓ multipoles, however, has a small (but observable) influence on the shape of the tail. We thus conclude that the value of $C(\theta \simeq 180^\circ)$ contains very interesting information concerning a possible *odd-even parity imbalance even for high- ℓ multipoles*.

4. Discussion

In spite of the high degree of isotropy in the CMB, certain anomalies have been found that create some tension with standard inflationary cosmology. The lack of long-range angular correlations beyond a maximum angle ($\theta_{\text{max}} \gtrsim 60^\circ$) is difficult to reconcile with the basic inflationary paradigm, which is founded on the principle of a slow-roll potential producing an accelerated expansion of over 60 e-folds. This maximum correlation angle instead allows only about 55 e-folds, well below the number required to solve the temperature horizon problem. Moreover, as shown in Melia & López-Corredoira (2017), the feature (i.e., k_{min}) that maps into such a maximum correlation angle also produces a zero-correlation plateau in the two-point angular correlation function at all larger angles.

Meanwhile, it has been known for some time that the angular power spectrum of the CMB favours a weighting of odd multipoles over even (see, e.g., Kim et al. 2012). This anomaly could mean a breakdown of the odd-even parity expected in the cosmological principle, so its study carries great interest. In this paper, we therefore sought to determine whether these two features, that is, k_{min} and an odd-even parity imbalance, are related, and/or whether both are required to produce the best fit to the *Planck* 2018 data.

We have incorporated a possible odd-even parity imbalance in our analysis by introducing nonuniform weighting factors that modify the C_ℓ coefficients in accordance with the parity statistic $Q(\ell_{\max})$. The outcome of this analysis has resulted in an excellent fit to the two-point correlation function, including the tail associated with the odd-parity dominance at $\theta \sim 180^\circ$. We have stressed that this angular region is influenced not only by the expected low- ℓ multipoles, but also to some degree by the high multipoles when the odd-even parity is broken.

At this stage, we can only speculate about a possible physical origin of k_{\min} and/or an odd-even parity imbalance. Certainly, in the context of slow-roll inflation, the cutoff signals the time at which inflation could have started. This is the principal reason why a nonzero value of this truncation to the primordial power spectrum is so restrictive for the ability of inflation to solve the temperature horizon problem while simultaneously producing the distribution of anisotropies seen in the CMB. A natural question that arises in this context is whether the presence of a cutoff, k_{\min} , should also impact the angular power spectrum itself. The answer appears to be yes, and it does so in a very intriguing way. It appears that the same value of u_{\min} required to optimize the fit to the angular correlation data also completely accounts for the ‘missing’ power seen in the low-multipole components (Melia et al. 2021). The fact that the same feature in $\mathcal{P}(k)$, that is, a $u_{\min} = 4.5 \pm 0.5$ (as we have found in this paper) can account for both empirically derived anomalies adds weight to its possible reality.

We here demonstrated that both k_{\min} and an odd-even parity imbalance are required to optimize the fit to the *Planck* 2018 data, however. So what could be the origin of this parity violation? There is no known mechanism that can produce such an imbalance due to inflation on its own. Prior to classicalization, all of the quantum fluctuations seeded in the early Universe and expanded during inflation were spherically symmetric (Melia 2021). Suggestions have therefore tended to focus on possible nonstandard beginnings or trans-Planckian issues. For example, topological models involving multiconnected universes have been invoked to account for the anomalous cold spot, or the aforementioned missing power at low multipoles (Efstathiou 2003; Land & Magueijo 2006). Although these models can lower the power of the small- ℓ multipoles, they apparently cannot create an asymmetry, however.

At face value, an odd-even parity imbalance might be viewed as a possible trans-Planckian effect (Brandenberger & Martin 2013), given that this is the first instance following the Big Bang when features measurable today would have emerged into the semi-classical Universe (Melia 2020). This topic touches on a broader issue related to the self-consistency of basic inflationary theory because the quantum fluctuations in the inflaton field would have been seeded in the so-called Bunch-Davies vacuum (Bunch & Davies 1978), well below the Planck scale. It is unclear, however, how or why quantum mechanics as we know it and general relativity could be used meaningfully to describe the evolution of these fluctuations on scales smaller than their Compton wavelength (see, e.g., Melia 2020). In other words, an odd-even parity imbalance may turn out to be a signature of trans-Planckian physics once a viable theory of quantum gravity is devised, but there is no evidence of this right now. Any oscillatory and sharp features in $\mathcal{P}(k)$ tend to become completely smeared out by the time the CMB power spectrum is produced (Bennett et al. 2011). Other possibilities may also include bouncing cosmologies (Agullo et al. 2020).

If confirmed to be of cosmological origin, an odd-parity dominance would violate the Cosmological Principle. Together

with the missing large-angle correlations, these two features could be an indication that new physics is required to modify the standard model accordingly, perhaps even leading to some exciting new discoveries about the origin and evolution of the Universe.

Regardless of its origin, however, the reality of an odd-over-even parity imbalance is becoming more firmly established in the analysis of the *Planck* data, making speculation such as this interesting to consider. Nevertheless, the existence of this asymmetry is by no means a certain indication that it originates from the CMB itself. As we indicated in the introduction, it may simply be due to an observational artifact. Recently, Creswell & Naselsky (2021b) discussed a link between the parity asymmetry and the low- ℓ peak anomaly, established in the presence of highly asymmetric regions in the sky, due to some foreground contamination in four regions near the Galactic plane ($[\ell, b] = [212^\circ, 21^\circ]$, $[32^\circ, 21^\circ]$, $[332^\circ, 8^\circ]$, and $[152^\circ, 8^\circ]$). This asymmetric distribution increases the odd-multipole power, while the deficit of symmetric regions leads to a corresponding deficit of even-multipole peaks. Therefore, the odd-even parity imbalance in the CMB could be explained, to a large statistical significance, as a consequence of an anomalous density of antipodal peaks in the sky once the dipole contribution from the motion of the Solar System is removed, without resorting to actual cosmological effects.

Having said that, we can safely conclude that our study in this paper establishes the compatibility of an infrared cutoff k_{\min} in the power spectrum with an odd-over-even parity imbalance, regardless of its origin, either cosmological or due to contamination, or an incorrect foreground subtraction. Our analysis has shown that both k_{\min} and the parity asymmetry are necessary in order to provide a best fit to the angular correlation function of the CMB.

5. Conclusion

This brief survey of possible causes of an odd-even parity imbalance is by no means exhaustive, but it is fair to conclude that a resolution of its origin will probably rely on new theoretical ideas. This stands in contrast to the meaning of k_{\min} , which can indeed in some way be attributed to the inflaton potential, $V(\phi)$. At least theoretically, there would be no obvious connection between this cutoff and the odd-even parity imbalance. Nevertheless, the observational evidence suggests that both are necessary to optimize the fit to the *Planck* 2018 data, as hinted also for the WMAP observations by the earlier work reported in Kim et al. (2012), although the WMAP measurements had a lower precision than the *Planck* 2018 observations, and these authors did not analyze in depth the two-point angular correlation function over its whole angular range, as we have done here for *Planck*.

Our main conclusion is that neither the odd-even imbalance nor the cutoff $k_{\min} = 4.5/r_d$ on their own and separately are sufficient to minimize the χ^2_{dof} of the $C(\theta)$ fit to the *Planck* 2018 data. Both are required, and while a nonzero k_{\min} may be attributed to an as yet undiscovered inflaton potential, the odd-even imbalance would appear to signal entirely new physics, if it is not simply due to contamination.

Acknowledgements. This work has been partially supported by Agencia Estatal de Investigación del Ministerio de Ciencia e Innovación under grant PID2020-113334GB-I00 / AEI / 10.13039/501100011033, by Generalitat Valenciana under grant PROMETEO/2019/113 (EXPEDITE), by the Center for Research and Development in Mathematics and Applications (CIDMA) through the Portuguese Foundation for Science and Technology (FCT - Fundação para a Ciência e a Tecnologia), references UIDB/04106/2020 and UIDP/04106/2020, by national funds (OE), through FCT, I.P., in the scope of the framework contract foreseen in the numbers 4, 5 and 6 of the article 23, of the Decree-Law 57/2016, of

August 29, changed by Law 57/2017, of July 19 and by the projects PTDC/FIS-OUT/28407/2017, CERN/FIS-PAR/0027/2019 and PTDC/FIS-AST/3041/2020. This work has further been supported by the European Union's Horizon 2020 research and innovation (RISE) programme H2020-MSCA-RISE-2017 Grant No. FunFiCO-777740 and by FCT through Project No. UIDB/00099/2020.

Schwarz, D. J., Copi, C. J., Huterer, D. & Starkman, G. D., 2016, CQG, 33, 184001

References

- Abramowitz, M. (Editor) & Stegun, I. A., 1970, *Handbook of Mathematical Functions: with Formulas, Graphs, and Mathematical Tables* (Dover Books on Mathematics, NY)
- Agullo, I., Kranas, D. & Sreenath, V., 2021, CQG, 38, 065010
- Aluri, P. K. & Jain, P., 2012, MNRAS, 419, 3378
- Bennett, C. L. et al., 2003, ApJS, 148, 97
- Bennett, C. L., Hill, R. S., Hinshaw, G. et al., 2011, ApJ, 192, 17
- Bouchet, F. R. et al., 2011, *CORe (Cosmic Origins Explorer) A White Paper*, (arXiv:1102.2181)
- Brandenberger, R. H. & Martin, J., 2013, CQG, 30, 113001
- Bunch, T. S. & Davies, P.C.W., 1978, Proc. R. Soc. A, 360, 117
- Creswell, J. & Naselsky, P., 2021a, JCAP, 2021, 103
- Creswell, J. & Naselsky, P., 2021b, submitted (arXiv:2105.08658)
- Di Valentino, E., Melchiorri, A. & Silk, J., 2021, ApJL, 908, L9
- Dong, F., Yu, Y., Zhang, J., Yang, X. & Zhang, P., 2021, MNRAS, 500, 3838
- Efstathiou, G., 2003, MNRAS Lett., 346, L26
- Errard, J., Feeney, S. M. et al., 2016, JCAP, Issue 03, article id. 052
- Guth, A. H., 1981, PRD, 23, 347
- Hanany, S. et al. [NASA PICO], 2019, *PICO: Probe of Inflation and Cosmic Origins*, (arXiv:1902.10541)
- Hinshaw, G. et al., 1996, ApJL, 464, L25
- Kazanas, D., 1980, ApJL, 241, L59
- Kim, J., Naselsky, P. & Hansen, M., 2012, Adv. Astron., 2012, 960509
- Land, K. & Magueijo, J., 2006, MNRAS, 367, 1714
- Linde, A. D., 1982, PLB, 108, 389
- Liu, J. & Melia, F., 2020, Proc. R. Soc. A, 476, 20200364
- López-Corredoira, M., Sylos Labini, F. & Betancort-Rijo, J., 2010, A&A, 513, A3
- López-Corredoira, M., 2017, Found. Phys., 47, 711
- Melia, F., 2014, A&A, 561, A80
- Melia, F., 2013a, A&A, 553, A76
- Melia, F., 2013b, CQG, 30, 155007
- Melia, F., 2014, A&A, 561, A80
- Melia, F. and López-Corredoira, M., 2018, A&A, 610, A87
- Melia, F., 2018, AJP, 86, 585
- Melia, F., 2019, EPJ-C, 79, 455
- Melia, F., 2020, Astron. Nachrichten, 341, 812
- Melia, F., 2020b, *The Cosmic Spacetime* (Taylor & Francis, Oxford)
- Melia, F., 2021, PLB, 818, 136632
- Melia, F., Ma, Q., Wei, J.-J. & Yu, B., 2021, A&A, 655, A70
- Melia, F., 2022, Astron. Nachrichten, in press (10.1002/asna.20224010)
- Mukhanov, V. F., 2005, *Physical Foundations of Cosmology* (Cambridge University Press, Cambridge)
- Panda, S., Aluri, P. K., Samal, P. K. & Rath, P. K., 2021, Astropart. Phys., 125, 102493 [erratum: Astropart. Phys., 130, 102582]
- Peebles, P.J.E., 1980, *The Large-Scale Structure of the Universe* (Princeton University Press, Princeton)
- Perivolaropoulos, L. & Skara, F., 2021, (arXiv:2105.05208)
- Planck Collaboration, Aghanim, N. et al., 2018, A&A, 641, A86
- Sachs, R. K. & Wolfe, A. M., 1967, ApJ, 147, 73
- Sanchis-Lozano, M. A., Sarkisyan-Grinbaum, E. K., Domenech-Garret, J. L. & Sanchis-Gual, N., 2020, PRD, 102, 035013
- Starobinsky, A. A., 1979, J. Exp. and Theo. Phys. Lett., 30, 682

Appendix A: Expansion factor following decoupling

The comoving distance to the last scattering surface may be written

$$r_d = c \int_{t_d}^t \frac{dt'}{a(t')}. \quad (\text{A.1})$$

The scale factor $a(t)$ determined from Friedmann's equations for an isotropic and homogeneous Universe made of matter (dust) and dark energy reads

$$\begin{aligned} \left(\frac{\dot{a}}{a}\right)^2 &= H_0^2 \left[\frac{\Omega_m}{a(t)^3} + \Omega_\Lambda \right] \\ \rightarrow a(t) &\sim \left(\sinh \left[\frac{3}{2} \sqrt{\Omega_\Lambda} H_0 t \right] \right)^{2/3}, \end{aligned} \quad (\text{A.2})$$

where $\Omega_\Lambda \simeq 0.7$ and H_0 denote the normalized dark matter density and Hubble parameter today, respectively. To simplify the notation, we define $\tilde{H} = (3/2) \sqrt{\Omega_\Lambda} H_0$, noting that in fact $\tilde{H} \simeq H_0$.

The proper (or physical) distance is given by

$$R_d = a(t) r_d, \quad (\text{A.3})$$

so that

$$R_d = \sinh^{2/3}[\tilde{H}t] \int_{t_d}^t \frac{dt'}{\sinh^{2/3}[\tilde{H}t']}. \quad (\text{A.4})$$

Changing to the variable $x = \sinh[\tilde{H}t]$, we obtain for the indefinite integral

$$\frac{1}{\tilde{H}} \int \frac{dx}{x^{2/3}(1+x^2)^{1/2}} = \frac{3 \sinh^{1/3} x}{\tilde{H}} {}_2F_1[1/2, 1/6; 7/6; -x^2]. \quad (\text{A.5})$$

Next, invoking the basic property of the hypergeometric series (Abramowitz & Stegun 1970),

$$\begin{aligned} {}_2F_1[a, b; c; z] &= (1-z)^{-a} {}_2F_1[a, b-c; c; z/(z-1)] \rightarrow \\ {}_2F_1[1/2, 1/6; 7/6; -x^2] &= \\ &= \frac{1}{(1+x^2)^{1/2}} {}_2F_1[1/2, 1; 7/6; x^2/(1+x^2)], \end{aligned} \quad (\text{A.6})$$

and reverting back to the original variable, we find the proper distance required to determine the maximum angle in Equation (5) to be

$$R_d = \frac{3 \sinh^{2/3}[\tilde{H}t]}{\tilde{H}} \times \left(\frac{\sinh[\tilde{H}t]^{1/3}}{\cosh[\tilde{H}t]} \times {}_2F_1\left[1/2, 1/6; 7/6; \tanh^2[\tilde{H}t]\right] - (t \rightarrow t_d) \right), \quad (\text{A.7})$$

where t here denotes the cosmic time of observation since the Big Bang. If the observation is today, then $t = t_0$ is to be identified with the present age of the universe.

Appendix B: Error due to the finite cutoff ℓ_{up}

In this appendix, we estimate the accuracy of the Legendre expansion of $C(\pi)$ over ℓ_{up} polynomials instead of infinity. For simplicity, we assume that the relation $C_\ell = 2\ell(\ell+1)$ is satisfied for all ℓ ; we therefore obtain $4\pi C(\pi) = 1/4$, as defined in Equation (3) for all ℓ from 2 to ∞ .

Thus, we may write

$$4\pi C(\pi) = 1/4 = \sum_{\ell=2}^{\ell_{\text{up}}} \frac{(2\ell+1)}{2\ell(\ell+1)} (-1)^\ell + \frac{(-1)^{\ell_{\text{up}}+1}}{2(\ell_{\text{up}}+1)}. \quad (\text{B.1})$$

This equation allows us to estimate the relative error made by neglecting polynomials of order higher than ℓ_{up} . In this work we set $\ell_{\text{up}} = 401$, so that the relative error is about 0.5%. Other effects such as BAO at large ℓ have been neglected throughout this analysis because they have very little or no influence on the large angles we are focused on in this paper.